

Figure 6 Transmission performance in dB of different filter configurations (IE3D). Conventional design without pin-pad resonators or coupling pad (dashed line); adding pin-pad resonators (dash-dotted line); coupling pad and pin-pad resonators (solid line)

Finally, we employ the coupling pad (see also Fig. 5) to create two more transmission zeros (solid lines in Figs. 6 and 7). The first transmission zero (Tz:1) is due to the parallel resonance that is formed by two components: (i) the electromagnetically coupled signal created between the resonators and (ii) the signal through the coupling pad. The second transmission zero (Tz:2) is due to the possible resonance through the fringe capacitance and inductance of the coupling pad with resonators and the ground plane. The dimensions of the various sections of the filter with coupling pad and pin-pad resonators are as follows: $\epsilon_r = 7.5$, $h = s + l = 0.5$ mm, $W = 0.6$ mm; resonators: length = 40 mm, spacing between the resonators = 1 mm, input/output line location = 4.5 mm from short-circuit end; pin-pad resonator 1: $x = y = 7.25$ mm, $l = 0.375$ mm, $d = 0.1$ mm; pin-pad resonator 2: $x = y = 8.6$ mm, $l = 0.375$ mm, $d = 0.1$ mm; coupling pad: length (along resonators) = 4 mm, width = 3 mm.

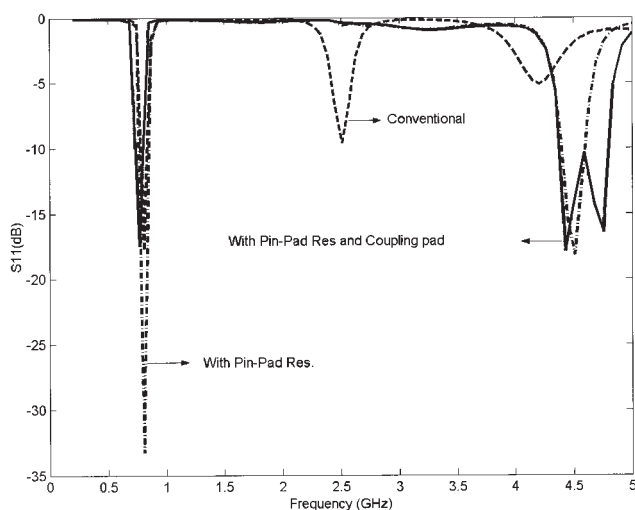


Figure 7 Reflection performance in dB of different filter configurations (IE3D). Conventional design without pin-pad resonators or coupling pad (dashed line); adding pin-pad resonators (dash-dotted line); coupling pad and pin-pad resonators (solid line)

Note that the results presented in Figures 6 and 7 have been obtained using IE3D[®] and, therefore, include all electromagnetic effects.

4. CONCLUSION

The equivalent-circuit model for grounded pin-pad resonators offers an attractive solution for the creation of transmission zeros in LTCC filter components. The determination of the resonance frequency or, alternatively, the pin-pad design for a given frequency is simple and straightforward. The process has been validated through an LTCC filter design, which was shown to achieve a transmission zero per pin-pad resonator. Hence, this design can be used to suppress a second passband. An additional coupling pad can be used to create additional transmission zeros closer to the passband. Both the equivalent-circuit model and the LTCC filter designs were verified through computations using the commercially available field solver IE3D[®].

REFERENCES

1. D.F. Sievenpiper, L. Zhang, F.J. Broas, N.G. Alexopoulos, and E. Yablonovitch, High-impedance electromagnetic surfaces with a forbidden frequency band, *IEEE Trans Microwave Theory Tech* 47 (1999), 2059–2074.
2. Y. Horii, A compact microstrip patch antenna having a 2-dimensional grounded-pad array embedded in an LTCC substrate, *IEEE AP-S Int Symp*, Columbus, OH, 2003, pp. 986–989.
3. Y. Horii, Filtering effects of grounded patches embedded in a microstrip line substrate, *IEICE Jpn Tech Rpt MWP02-3* (2002), 15–22.
4. B.C. Wadell, *Transmission line design handbook*, Artech House, Boston, 1991.
5. G. Matthaei, L. Young, and E.M.T. Jones, *Microwave filters, impedance matching networks and coupling structures*, Artech House, Boston, 1980.
6. L.H. Hsieh and K. Chang, Compact elliptic function lowpass filters using microstrip stepped impedance hairpin resonators, *IEEE Trans Microwave Theory Tech* 51 (2003), 193–199.
7. T. Ishizaki, M. Fujita, H. Kagata, T. Uwano, and H. Miyake, A very small dielectric planar filter for portable telephones, *IEEE Trans Microwave Theory Tech* 42 (1994), 2017–2022.
8. K. Rambabu and J. Bornemann, Simplified analysis technique for the initial design of a class of LTCC filters, *IEEE Trans Microwave Theory Tech* 53 (2005), 1787–1791.

© 2005 Wiley Periodicals, Inc.

DESIGN OF PIN DIODE CONTROLLED VARIABLE ATTENUATOR USING SLOW WAVE MICROSTRIP LINES

Kae-Oh Sun and Daniel van der Weide

Department of Electrical and Computer Engineering
University of Wisconsin
1415 Engineering Drive, Madison, WI

Received 18 May 2005

ABSTRACT: We describe a simple PIN-diode-controlled variable attenuator that employs a 0-dB branch-line directional coupler, and present a method to reduce the size using slow-wave microstrip lines. At the center frequency, the attenuation monotonically varied from 0.7 to 23 dB with the control voltage. By using slow-wave microstrip lines, we achieve a 60% size reduction compared to a conventional structure. © 2005 Wiley Periodicals, Inc. *Microwave Opt Technol Lett* 47: 323–327, 2005; Published online in Wiley InterScience (www.interscience.wiley.com). DOI 10.1002/mop.21159

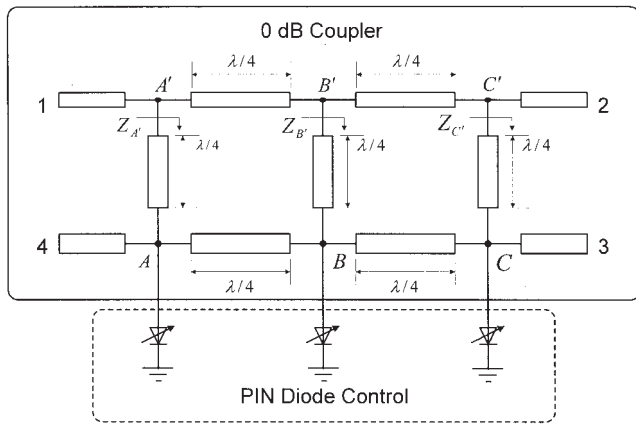


Figure 1 Attenuator schematic diagram (all lines are $Z_0 = 50\Omega$)

Key words: PIN diode; variable attenuator; slow wave

1. INTRODUCTION

Variable attenuators are used to control power transmission, and they have applications in devices modulators, automatic gain-control circuits, and radar systems. PIN diodes are commonly used as the control element in variable attenuators because of their speed and ease of design. Many types of variable attenuators using PIN diodes have been presented: π attenuators, resistive line attenuators, bridged-T attenuators, hybrid coupled attenuators, and others [1]. The hybrid coupled attenuator is frequently used when reflected power must be minimized, and a double hybrid coupled attenuator is especially preferred due to its wider bandwidth, although it requires a larger area than a single hybrid coupled attenuator. There can be several ways to reduce the size of couplers. Lumped-element couplers are ready examples [2], but lumped inductors and capacitors with the required values and high-quality factors are not usually available for use in MICs or MMICs. Slow-wave transmission lines are also promising candidates for size reduction [3, 4], but many employ complex 3D structures that may be difficult to fabricate. In this paper, we present a novel variable attenuator employing a 0-dB branch-line directional coupler [5] using 2D slow-wave microstrip lines that is smaller in area but has comparable or better performance than a double hybrid coupled attenuator.

2. ATTENUATOR CIRCUIT DESIGN AND ANALYSIS

A PIN diode is a PN junction diode that has an intrinsic layer between its P-type and N-type layers. The PIN diode behaves as an ordinary PN junction diode at low frequencies, but at high frequencies it behaves as a resistor whose value can be controlled by current. Using this resistive characteristic, we constructed a variable attenuator by combining the PIN diode with a 0-dB branch-line coupler (Fig. 1).

Ideally, the resistance of the PIN diodes can be varied from infinity to zero, which means that nodes A, B, and C can be floating or, conversely, connected to ground. When the nodes are floating, the whole circuit acts as a 0-dB coupler itself, and the incident power on port 1 is transferred to port 3 without any attenuation or reflection. However, when nodes A, B, and C are grounded, the input resistances Z'_A , Z'_B , and Z'_C as seen from A' , B' , and C' to the branches, approach infinity.

Applying an even-odd mode analysis for the infinite resistance case, we can obtain the ABCD matrices as follows:

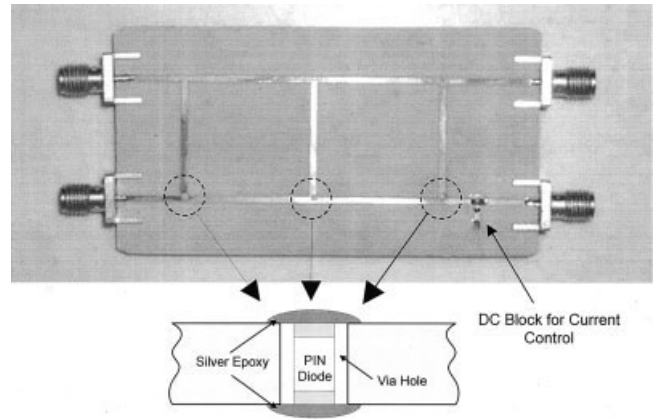


Figure 2 Layout and fabrication details of the attenuator

$$\begin{bmatrix} A & B \\ C & D \end{bmatrix}_e = \begin{bmatrix} 1 & 0 \\ j & 1 \end{bmatrix} \begin{bmatrix} 0 & j \\ j & 0 \end{bmatrix} \begin{bmatrix} 1 & 0 \\ j & 1 \end{bmatrix} \begin{bmatrix} 0 & j \\ j & 0 \end{bmatrix} \begin{bmatrix} 1 & 0 \\ j & 0 \end{bmatrix} = \begin{bmatrix} 0 & -j \\ -j & 0 \end{bmatrix} \quad (1)$$

$$\begin{bmatrix} A & B \\ C & D \end{bmatrix}_o = \begin{bmatrix} 1 & 0 \\ -j & 1 \end{bmatrix} \begin{bmatrix} 0 & j \\ j & 0 \end{bmatrix} \begin{bmatrix} 1 & 0 \\ -j & 1 \end{bmatrix} \begin{bmatrix} 0 & j \\ j & 0 \end{bmatrix} \begin{bmatrix} 1 & 0 \\ -j & 0 \end{bmatrix} = \begin{bmatrix} 0 & j \\ j & 0 \end{bmatrix} \quad (2)$$

From these equations, the amplitude of the emerging wave at each port in Figure 1 is $B_1 = B_2 = B_4 = 0$, $B_3 = j$, and all the incident power is transferred to port 3. The power transferred in the zero resistance case can be derived qualitatively. The power transferred

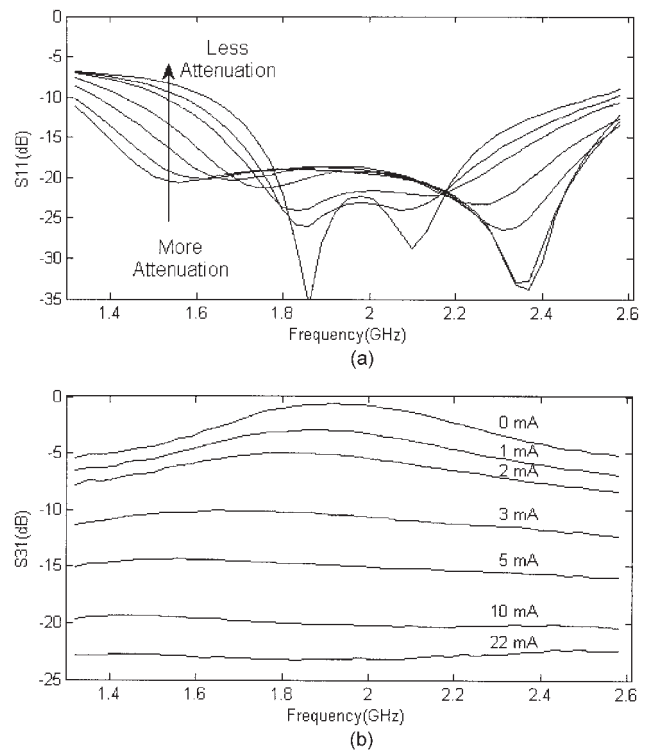


Figure 3 (a) Equivalent measured reflection and (b) attenuation vs. control current

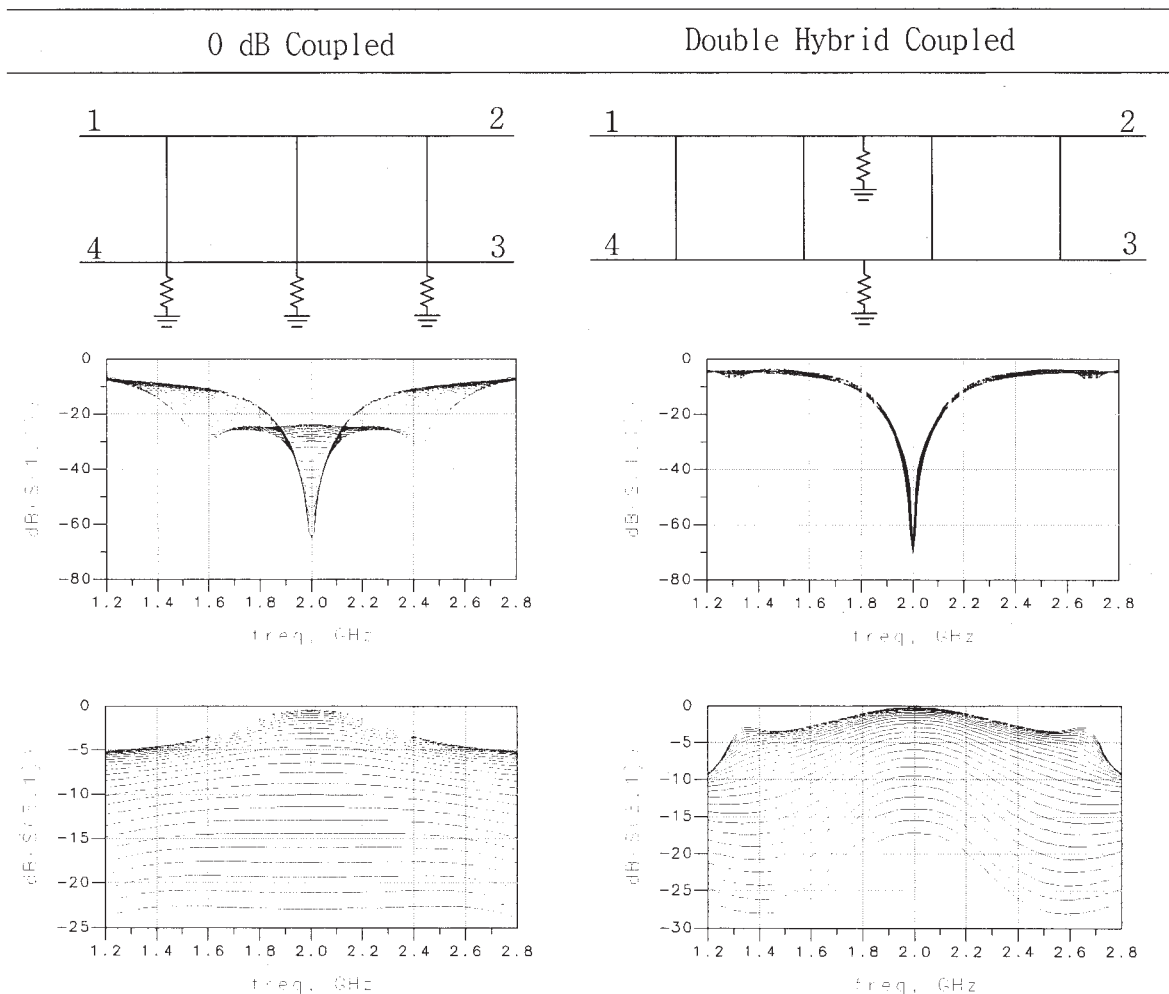


Figure 4 ADS-simulated performance of our attenuator vs. a double hybrid coupled attenuator

in the zero resistance case can be derived qualitatively. Intuitively, it is clear that all the incident power is transferred to port 2 because the input impedances, as seen from nodes A' , B' , and C' , approach infinity due to the branches having quarter-wave lengths and each branch being grounded. Thus, no power is transferred to port 3 and 4, nor is any power reflected back to port 1.

3. FABRICATION AND MEASUREMENT RESULTS OF THE VARIABLE ATTENUATOR

The most important performance-design consideration is to provide a good ground to the PIN diodes when their resistances are minimized. In order to make the shortest path to the ground plane from the microstrip line, we selected a thin board ($\epsilon_r = 3.38$, dielectric thickness = 0.2 mm) and directly inserted the PIN diodes through via holes, as shown in Figure 2. For this design, we used MA4FCP200 flip chip PIN diode manufactured by MACOM®. According to the manufacturer's data sheet, the minimum resistance of the PIN diodes used was 5.2Ω at 1 MHz and 4.2Ω at 10 GHz with 10-mA current.

The measured circuit performance is shown in Figure 3. As seen in Figure 3(b), the attenuation-control current plot remains relatively flat throughout the whole frequency range, so the bandwidth is mainly determined by the reflection characteristics. S_{11} is shown in Figure 3(a). Figure 4 shows the ADS simulation results of a 0-dB coupled attenuator and a double hybrid coupled attenuator for comparison, disregarding the discontinuities of each junc-

tion. In the circuit schematics, port 1 is the input and port 3 is the output. As can be seen in this figure, a 0-dB coupled attenuator has advantages over a double hybrid coupled attenuator, such as smaller size, wider bandwidth (due to the lower input reflection), and larger attenuation range.

4. SLOW-WAVE MICROSTRIP-LINE DESIGN AND MOMENTUM SIMULATION RESULTS

The characteristic impedance Z_0 and phase velocity v_p of a transmission line are well known as follows:

$$Z_0 = \sqrt{\frac{L}{C}}, \quad (3)$$

$$\lambda = \frac{v_p}{f}, \quad (4)$$

$$v_p = \frac{1}{\sqrt{LC}}. \quad (5)$$

From Eqs. (3–5), it follows that the wavelength can be decreased while the characteristic impedance is kept unchanged by increasing L and C with the same ratio. Yet both the inductance and capacitance of the microstrip are related to line width; inductance increases with decreasing line width, whereas capacitance in-

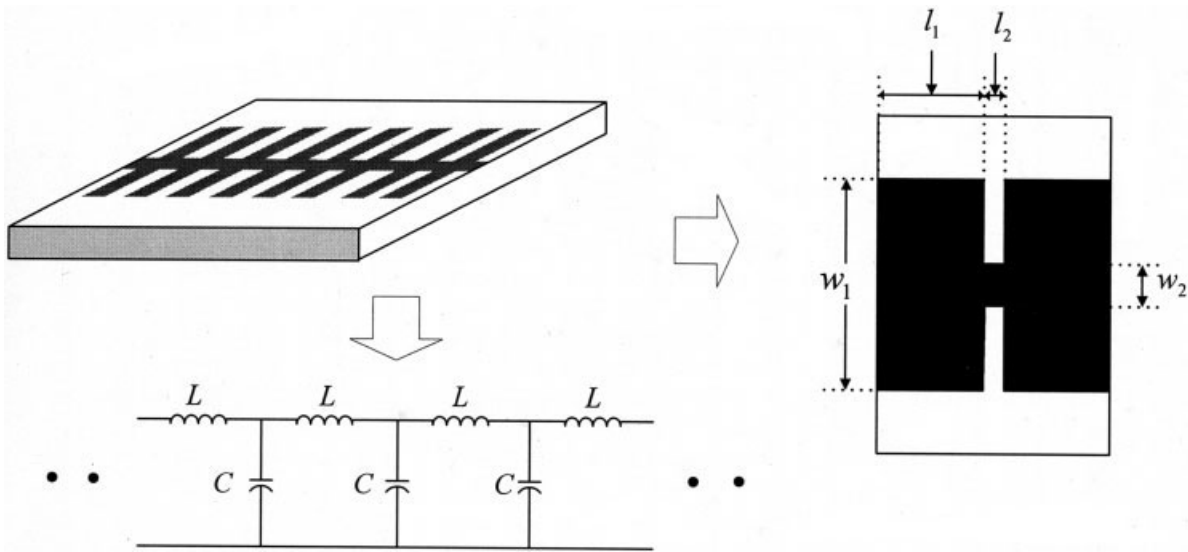


Figure 5 Equivalent circuit of a transmission line with discontinuities

creases with increasing line width. For a given electrical length, the physical length of a transmission line, such as a microstrip, can be reduced by using a slow-wave structure. In this paper, we designed a slow-wave transmission line by employing discontinuities along it. A step discontinuity provides the line with additional inductance and capacitance. The discontinuous transmission line is made by placing a wide line and a short line and a narrow and short line in turn. Throughout this paper, those lines will be called a capacitive line and an inductive line, respectively. A transmission line with the repeated discontinuities can be modeled as shown in Figure 5. In this equivalent circuit, L is equal to $L_c + L_i + L_d$ and C is equal to $C_c + C_i + C_d$. The notations used here are defined as follows:

- L_c, C_c = inductance/capacitance per unit length, which is induced by a capacitive line;
- L_i, C_i = inductance/capacitance per unit length, which is induced by an inductive line;
- L_d, C_d = inductance/capacitance per unit length, which is induced by discontinuities.

The inductance and the capacitance induced by discontinuities are dependent on the board thickness and the line width. For a step discontinuity, both the inductance and capacitance increase as the width ratio of the two connected lines increases [6]. Our circuit was designed using a board with 0.2-mm thickness, whose dielectric constant is 3.38 and ADS Momentum simulations were run.

TABLE 1 Distributed Element Values Per mm of Discontinuous and Continuous Lines (units: nH for Inductance, pF for Capacitance)

Discontinuous 50Ω line					
L_c	L_i	L_d	C_c	C_i	C_d
0.07	0.26	0.2	0.116	0.026	0.07
Continuous 50Ω line					
L					C
0.27					0.108

The capacitive line width W_1 , capacitive line length l_1 , inductive line width W_2 , and inductive line length l_2 of the discontinuous lines with 50Ω characteristic impedances are $W_1 = 1.3$, $l_1 = 0.1$, $W_2 = 0.1$, $l_2 = 0.1$, respectively (unit: mm).

Distributed inductances and capacitances per mm of discontinuous lines with these dimensions and continuous lines are shown in Table 1 for comparison. All values are distributed for a 1-mm length. Both of inductive lines and capacitive lines are 0.1-mm long in this example. Therefore, this table shows the values for a 0.5-mm inductive line and a 0.5-mm capacitive line to make a 1-mm discontinuous line. L_d and C_d should also include the coupling effects between capacitive lines when they are very close. Many studies have been done to analyse step discontinuities [7]. However, most of them assumed long transmission lines at both sides of a discontinuity, and they cannot be directly used when discontinuous sections are close. So, instead of using those methods, L_d and C_d in Table 1 were calculated by measuring image impedance. Then, the phase velocity of a discontinuous transmission line is given by

$$v_p = \frac{1}{\sqrt{(L_c + L_i + L_d)(C_c + C_i + C_d)}}$$

So, from Table 1 it is obvious that the discontinuous transmission line is much shorter than the conventional transmission line for the same electrical wavelength.

Figure 6 shows the layout of the compact 0-dB coupler designed using slow-wave microstrip lines and Figure 7 shows the

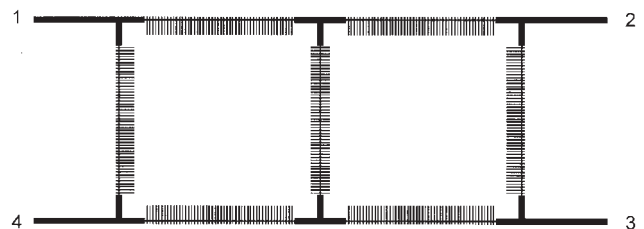


Figure 6 Layout of the compact 0-dB coupler

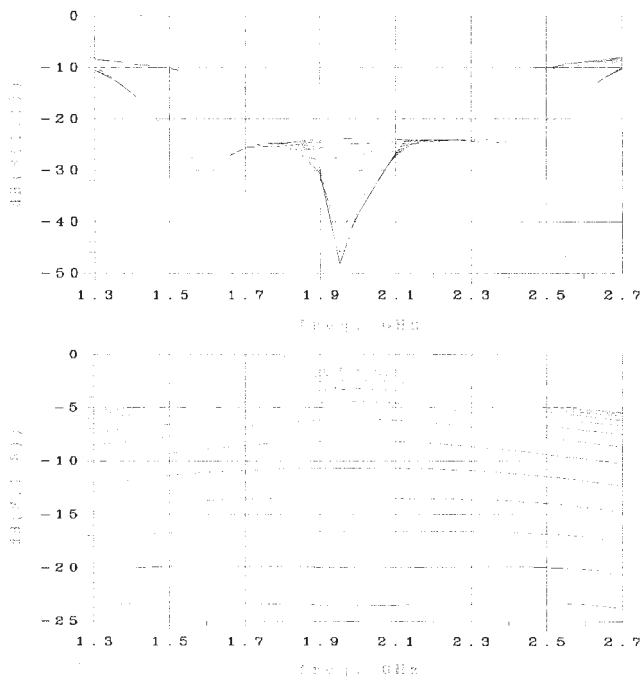


Figure 7 Simulated reflection (top) and attenuation (bottom) vs. PIN-diode resistance

ADS Momentum simulation results for the reflection and the attenuation as PIN diode resistances are changed. These results are comparable with the experimental results of Figure 3. The area of the variable attenuator using conventional microstrip lines is 105 mm² versus 39 mm² for the compact one, more than 60% reduction in size.

5. CONCLUSION

We have described the design and performance of a PIN-diode-controlled variable attenuator employing a 0-dB branch-line directional coupler and a miniaturizing technique. Due to the low reflected power of the coupler, the attenuator has excellent input and output impedance matching. At 1.9 GHz, it has an attenuation range between 0.7 and 23 dB, which can be further improved by using a thinner substrate and PIN diodes with lower series resistances. This modification would result in the control locations *A*, *B*, and *C* (shown in Fig. 1) being nearer to an ideal ground when the PIN diodes are turned on. The size of the variable attenuator was reduced by 60% using the proposed slow-wave microstrip-line design technique.

REFERENCES

1. AN-922 Applications of PIN diodes, Hewlett Packard, 1997.
2. Y.C. Chiang, and C.Y. Chen, Design of a wideband lumped-element 3-dB quadrature coupler, *IEEE Trans Microwave Theory Tech* 49 (2001), 476–479.
3. G.A. Lee, H.Y. Lee, and F.D. Flaviis, Perforated microstrip structure for miniaturizing microwave devices, *IEE Electron Lett* 38 (2002), 800–801.
4. J. Martel, R.R. Boix, and M. Horno, Equivalent circuits for MIS microstrip discontinuities, *IEEE Microwave Guided Wave Lett* 3 (1993), 408–410.
5. D. Kholodniak, G. Kalinin, E. Vernoslova, and I. Vendik, Wideband 0-dB branch-line directional couplers, *IEEE MTT-S Int Microwave Symp Dig* 3 (2000), 1307–1310.

6. M.J. Webster, B. Easter, and J.S. Hornsby, Accurate determination of frequency dependent three element equivalent circuit for symmetric step microstrip discontinuity, *IEE Proc Microwaves, Antennas and Propagation* 137 (1990), 51–54.
7. A.F. Thomson and A. Gopinath, Calculation of microstrip discontinuity inductances, *IEEE Trans Microwave Theory Tech* 23 (1975), 648–655.

© 2005 Wiley Periodicals, Inc.

WIDEBAND MAGIC-T COUPLER USING AN ASYMMETRIC COPLANAR STRIPLINE OR COPLANAR WAVEGUIDE RING STRUCTURE

Min-Hua Ho

Electronic Engineering Dept.
National Changhua University of Education
1, Jin-De. Rd.
50007 Changhua City, Taiwan

Received 16 May 2005

ABSTRACT: A uniplanar wide-band magic-T circuit using an asymmetric coplanar-stripline (ACPS) or a coupler waveguide (CPW) ring circuit is proposed. Both types of structure exhibit a uniplanar configuration which reduces the circuit complexity and manufacturing cost. A phase-reverse section is built in the E-arm branch of the circuits to obtain the function of a magic-T operation. The ACPS- and CPW-ring magic-T couplers have measured bandwidths of 4.4 and 4.6 GHz, respectively, with acceptable amplitude and phase imbalances. © 2005 Wiley Periodicals, Inc. *Microwave Opt Technol Lett* 47: 327–330, 2005; Published online in Wiley InterScience (www.interscience.wiley.com). DOI 10.1002/mop.21160

Key words: ACPS ring; CPW ring; magic-T; wideband; uniplanar

1. INTRODUCTION

Magic-T couplers (also known as 180° hybrid couplers) are fundamental components in power combiners/dividers and balanced mixer circuits [1, 2]. To achieve good performance of a magic-T circuit requires a wide bandwidth, a low power-dividing/combining loss, small amplitude and phase imbalances, high isolations between different ports, and sometimes the circuit compactness. The magic-T was first built by a rectangular waveguide T-junction [3]. In spite of this waveguide's ultra-low loss property, it is considered to be costly and cumbersome due to its bulky and inflexible structure, which hinders it from finding applications in modern commercial microwave systems that require circuit compactness, light weight, and low cost. The planar structured magic-T circuits [4–6] which use a ring structure in the design have been reported in the past decade. They have the advantages of a wide bandwidth, low profile, low cost, light weight, and easy mass production. In [4, 5], various 180° phase-reverse sections composed of varieties of CPW and slotline combined structures are embedded in hybrid ring configurations to achieve the magic-T function and a wideband property. In [6], the circuit was constructed by coplanar-stripline ring (CPS ring) with the phase-reverse section made of a twisted CPS structure also embedded in the ring structure.

In this paper, a uniplanar magic-T circuit using an asymmetric coplanar-stripline (ACPS) ring or a CPW ring structure is presented. The phase-reverse section of the circuit is built in the end of the E-arm branch by using vias and a short metal strip on the opposite side. The proposed magic-T ring coupler has character-